ORIGINAL PAPER





Utilizing bioprinting for hydrogel-based electric double-layer capacitor fabrication

Bianca Seufert¹ · Sylvia Thomas · Arash Takshi¹

Received: 20 November 2023 / Accepted: 11 February 2024 / Published online: 4 March 2024 © The Author(s), under exclusive licence to The Materials Research Society 2024

Abstract

The mass production and use of Li batteries have raised serious concerns about their impact on the environment. Supercapacitors are an alternative energy storage device. This paper addresses a new approach to fabricating supercapacitors using the BioX6 Bioprinter from Cellink. A series of experiments were conducted to derive a conductive bioink capable of being implemented as a viable material for energy storage devices. This bioink in conjunction with a gel electrolyte was utilized for the fabrication of supercapacitors in a planar structure. This study utilizes the VersaStat 4 Potentiostat to measure each capacitors' response. Devices with capacitances as high as $53.52 \,\mu\text{F}$ were fabricated and tested. The results of this study show the feasibility of using the bioprinting method for fabricating prototype storage devices.

Introduction

The fast growth in the wearable and medical electronics industries encourages designing customized and flexible circuits for various applications. However, the bulky structure of traditional batteries may limit the flexibility of the final product. To address this challenge, printed energy storage devices can be a solution for synthesizing thin and flexible products. With Li batteries raising serious concerns about their impact on the environment, printable supercapacitors made with environmentally friendly and benign materials is preferable. Advantages of supercapacitors are their ability to be charged and discharged at high rates with high power densities and a long cycling stability. However, due to the high material cost and low specific energy characteristic, supercapacitors are not capable of replacing batteries just yet [1]. There are three different types of supercapacitors: electric double-layer capacitors (EDLC) supercapacitors, pseudo-supercapacitors, and hybrid-supercapacitors. These categories are determined by their respective energy storage principles. EDLCs use electrostatic interactions to hold charges. Pseudo-supercapacitors utilize redox reactions for charge storage and hybrid-supercapacitors utilize both methods. For the scope of this paper, however, only EDLCs will be discussed.

Electric double-layer capacitors (EDLCs)

As an electrochemical device, EDLCs are made up of two electrodes and an electrolyte that separates the two electrodes. The principle behind EDLCs is the use of electrostatic interactions to form two layers of charge across the electrode–electrolyte interface. On the electrolyte side, the arrangement of the ions forms the Helmholtz and diffusion layers. The Helmholtz layer form between the electrodes surface and the electrolyte. The electrons from the electrode and the ions from the electrolyte are separated by solvent molecules that act as the dielectric of the capacitor. The capacitance results from the charge accumulation within the double layer. The capacitance is limited by the amount of charge that can physically fit within the double layer.

Given that this type of supercapacitor relies heavily on electrochemical interactions, the materials used to create both the electrodes and electrolyte are incredibly important. Activated carbon is a common material utilized for electrode fabrication because of its larger surface area and electrolytes that can be made up of a wide range of ionic liquids [2]. The overall nature of an EDLC can be treated as an electrochemical cell which facilitates the use of electrochemical measurements, most notably cyclic voltammetry, to study these cells.

Department of Electrical Engineering, University of South Florida (USF), 4202 E. Fowler Ave, Tampa, FL 33620, USA



Fabricating EDLCs

Furthermore, traditional EDLC fabrication isn't exactly eco-friendly. With aprotic electrolytes that including various metals and chemicals that contribute to electronic waste, researchers are approaching new ways to reduce this by finding more environmentally friendly ways to produce devices such as EDLCs by synthesizing protic electrolytes for conductive inks and hydrogels that are biodegradable and environmentally safe because they are water based [2].

The idea of printing electrodes has been around for a few years now. By converting over to liquid compounds, one can avoid hard metals and plastics while also choosing biodegradable alternatives. The resulting printed components also provide flexibility that traditional solid-state devices lack. Researchers from Boise-State University are utilizing these advantages to fabricate inkjet-printed flexible electrodes for repeatable electrochemical responses. They used graphene-based ink to create electrodes with viable electrochemical results [3]. In addition to printing electrodes, a second group of researchers applied these electrodes for pH sensing with accurate results and were easily able to get repeatable results [4].

Moreover, while standard printing techniques can be employed for printing electrodes another printing technique has come to light that can print a capacitor in its entirety. This unique technique is called bioprinting. While this fabrication process is most associated with medical device fabrication, bioprinting can bring about a truly new approach to capacitor fabrication. Bioprinting provides versatility with a wide range of available biodegradable and biocompatible materials. Bioprinting also allows for unique geometries and patterns to be printed. Several researchers have conducted studies in conductive bioinks to advance the development of biodegradable, biocompatible, and flexible electronics. Many researchers are utilizing natural hydrogels such as alginate or synthetic polymers, such as poly(ethylene glycol), as bioinks due to their ionic nature and low cost [5–7].

Materials and methods

Materials and equipment

Carbon nanofibers (CNFs), indium tin-oxide (ITO)-coated polyethylene terephthalate (PET), and H₃PO₄ were

purchased from Sigma Aldrich. Polyvinyl-alcohol (PVA) from Alfa Aesar was used to make the gel electrolytes. Polypropylene, PPO (a.k.a Cellink's START bioink), was purchased from Cellink. The BioX6 Bioprinter from Cellink was used to fabricate the electrodes and print the electrolyte in some samples. VersaStat 4.0 potentiostat and a Kiethley 2602 equipped with a custom-made 4-probe setup were used for the electrochemical and conductivity measurements, respectively.

Electrode bioink and gel electrolyte

As shown in Table 1, the bioink used for synthesizing the electrodes for the EDLC was created by mixing different amounts of CNFs (0, 0.06, and 0.1 g) with 3 ml polypropylene (PPO). The concentration of CNFs suspended within the PPO was determined by trial and error. The bioink was assembled by adding both ingredients to a beaker and manually mixing them together for 2–3 min. Then the mixture was loaded into a bioprinter cartridge to be used immediately. Samples with different amounts of CNFs at the thickness of ~0.24 mm were printed on the electrodes designed for the 4-probe measurements.

The gel electrolyte was prepared by mixing together 0.5 mL of H_3PO_4 , 0.75 g of PVA, and 5 mL of DI water. The electrolyte was assembled by placing all ingredients into a beaker with a magnetic stirrer. The beaker was then sealed with parafilm and left to heat at $90 \,^{\circ}\text{C}$ and stir at $450 \,^{\circ}\text{C}$ pm for $4 \,^{\circ}\text{L}$. Then the beaker was removed from the heat and left at room temperature for $48 \,^{\circ}\text{L}$ h to reach the gel consistency needed for the bioprinter.

Printing EDLC samples

Figure 1 shows the fabrication steps of the supercapacitors. As shown, a rectangle piece (6 cm×2 cm) of ITO electrode was taped on a glass slide with two pieces of copper tape. Using the 0.1 g CNF-based ink, two square-shaped (2 cm×1.5 cm) patterns were printed on the ITO electrode before cutting the ITO electrode to separate the two electrodes. In some samples, 0.5 ml of the PVA electrolyte was applied manually to cover both printed CNF electrodes. The rest of the samples were made by printing the PVA gel on top of the electrodes. Hot glue was used to seal the devices with a blank glass slide covering the electrolyte. In total,

Table 1 Trial bioink compositions with corresponding average conductivity & pritning parameters

Bioink Version	Composition	Conductivity (mS)	Pressure	Printing Speed	Nozzle Gauge
1	3 mL PPO	.19 mS	20 kPa	20 mm/s	22G
2	0.06g CNF+3 mL PPO	.21 mS	85 kPa	5 mm/s	17G
3	0.1 g CNF+3 mL PPO	.39 mS	90 kPa	5 mm/s	17G



520 B. Seufert et al.

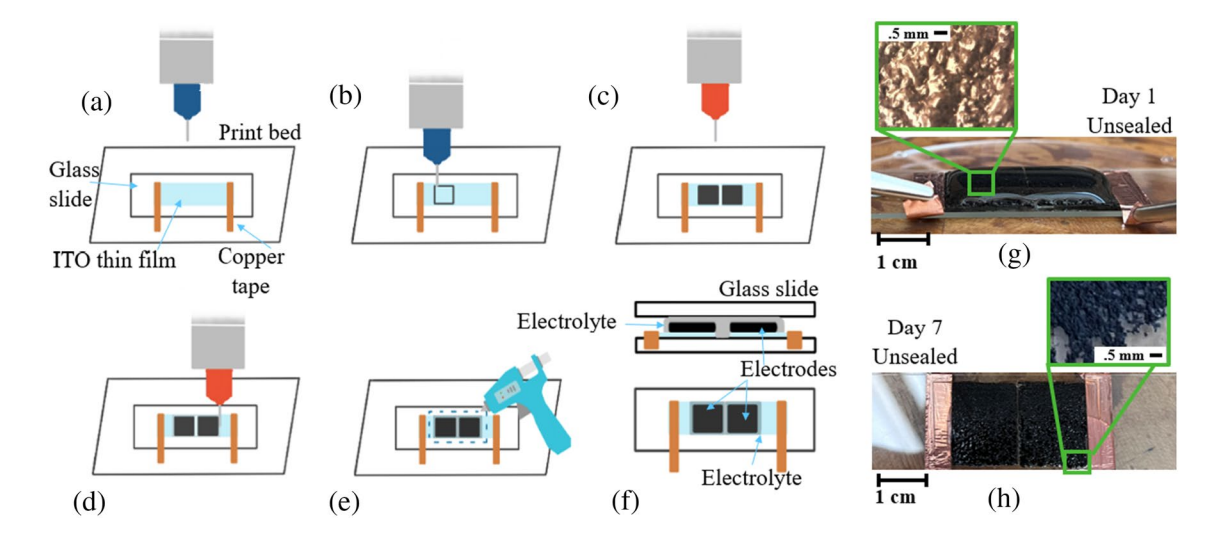


Fig. 1 Bioprinting process schematic. (a) Sample substrate before bioprinting electrodes. (b) Printing of electrodes. (c) Cut substrate between electrodes and load electrolyte bioink. (d) Print electrolyte

over electrodes. (e) Seal newly printed sample with hot glue and another glass slide. (f) Sample diagram (g) Freshly printed unsealed sample (h) Unsealed sample after 7 days

four different types of devices were fabricated and tested that are referred to as samples 1—4 from now on. Sample 1 had the electrolyte manually applied over the top of the electrodes. Sample 2 had the electrolyte bioprinted over the top of the electrodes. Sample 3 had the electrolyte manually applied over the electrodes and then the sample was sealed. Sample 4 had the electrolyte bioprinted over the top of the electrodes and then sealed the same as sample 3. Each electrode weighed approximately 0.20 g. Once each sample was finished, it was put through a series of electrochemical tests approximately 10 min after being printed/sealed. Optical images of the electrodes and devices were taken and are presented in Fig. 1. It should be noted that due to the wet nature of the printed electrodes, we could not use the scanning electron microscopy (SEM) method to characterize the electrodes.

Results

To study the capacitive behavior of the printed samples, cyclic voltammetry (CV) experiments were conducted using the two-probe configuration with a scan rate of 50 mV/s. Since the electrolyte was an aqueous based gel, the voltage range was limited to \pm 1.0 V to avoid water electrolysis. The results of these printed cells can be seen in Fig. 2 & Table 2 for reference. While in an ideal EDLC, a square-shaped CV loop is expected, our previous study on PVA gels suggests that the CV results may show oxidation and reduction peaks due to the redox behavior of the gel [8]. Such peaks appeared well in Sample 3 with manually applied electrolyte and sealing. The redox peaks were also observed in the

other samples, but the amplitude of the peaks was relatively small in Samples 1, 2, and 4. Additionally, the tilted loops in those samples suggest that the resistive behavior of the electrochemical cell is largely affecting the double-layer charge storage. Furthermore, the non-symmetrical shape of the loop with current tails (particularly in Fig. 2a and b) implies direct charge transfer between the electrode and the electrolyte, likely due to the defects on the printed electrodes providing direct paths for the ions to reach the current collector layer beneath the printed electrodes. Considering that one electrode can have more defects than the other; as observed, the CV loops can be non-symmetrical around 0.0 V. Since the materials used in all the samples and their geometries were the same, the difference between different samples can be attributed to the difference in the structure of the films due to different gel application methods and the effect of sealing the devices after the fabrication. Nevertheless, the loop-shaped results demonstrate the capacitive behavior of the samples. Also, it is demonstrate in Fig. 2e that Sample 3 had the largest capacitance. As the optical images in Fig. 1 show, because of the viscous nature of the printed materials, the electrodes could not keep their original printed shape and started to spread. That may explain why the fabricated devices did not show the ideal capacitive CV loop. More importantly, we noticed that this spreading effect changes the capacitance of the devices over time. Hence, we further studied the samples by measuring their capacitances over 7 days. After conducting measurements on each cell and reviewing the results, it became clear that day 2 results for samples 1 and 2 were drastically out of character with the overall results. Due to this anomaly, day 2 results have been excluded from Table 2.



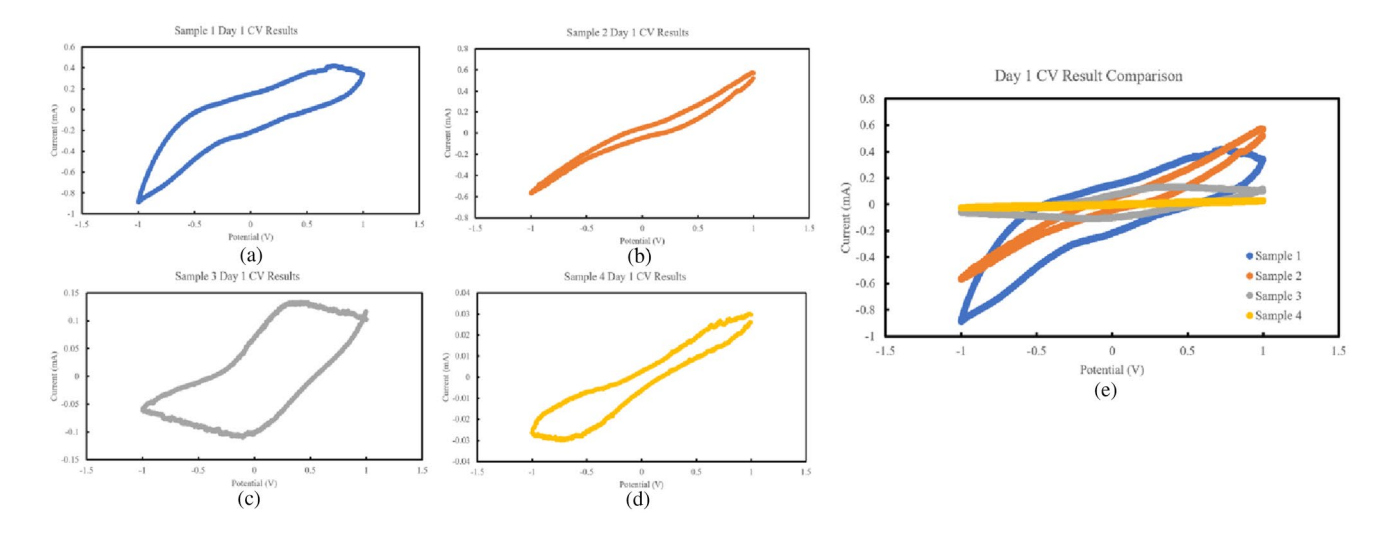


Fig. 2 (a) CV of Sample 1 (manually applied electrolyte and no seal), (b) CV of Sample 2 (bioprinted electrolyte and no seal), (c) CV of Sample 3 (manually applied and sealed), (d) CV of Sample 4 (bioprinted electrolyte and sealed), (e) Comparison of the CV results of all samples

Table 2 Calculated capacitances

Capacitance (μF)							
Day	Sample 1	Sample 2	Sample 3	Sample 4			
1	46.95	37.43	53.52	5.38			
3	31.03	0.22	0.20	0.03			
4	19.62	0.59	0.21	0.03			
5	23.05	0.12	0.20	0.02			
6	15.62	0.41	0.17	0.06			
7	13.66	0.59	0.16	0.05			

Furthermore, based on these results after the first day, each cell experiences a significant drop in capacitance. Another notable observation is that the sealed samples, samples 3 and 4, did not maintain the capacitance of day 1 as might be expected. Considering that the electrolyte doesn't evaporate nearly as fast as the electrolyte with the unsealed samples, this is an intriguing result.

Discussion

Moreover, each cell experienced a significant initial drop in capacitance after the first day of measuring; however, only the sealed samples continued to maintain relatively the same capacitance as day 3 throughout the week. The unsealed samples, however, fluctuated throughout the week as the layers were deformed due to the viscus nature of the printed materials. All the samples were left uncovered at room temperature. Also, there is a likelihood of sample contamination or moisture absorption/loss over time for the unsealed sample which could account for this fluctuation.

When comparing capacitances from Table 2, it is made apparent that even though the electrolyte was bioprinted on samples 3 and 4, it didn't necessarily result in a higher capacitance beyond first day measurements. Samples 1 and 3 both show a higher capacitance than samples 2 and 4 with sample 4 being an outlier. This difference in sample capacitances could have occurred due to damage to the electrodes during the printing of the electrolyte. The force of extrusion of the electrolyte could have resulted in compression of the highly malleable electrodes decreasing the surface area of the CNFs suspended in the bioink.

Another interesting development is that the sealed samples did not show higher capacitances. Given that the bioprinted electrolyte provided a considerably more even application of the electrolyte to be absorbed by the electrodes, this didn't result in a higher capacitance as might have been expected. The first measurement of Sample 3 proved to be the largest reading at 53.52 µF. However, the remaining measurements were significantly less. This demonstrates that sealing the cell doesn't necessarily mean it will maintain the same level of capacitance over time. The decreased capacitance could be from the sealing process, specifically, the pressure of applying the glass slide could have damaged the electrodes' internal structure. This, however, did protect the sample over a 7-day period resulting in minor fluctuations rather than larger fluctuations as seen in sample 1. Table 2 also demonstrates the aging effect of each cell over a 7-day period. This helps put in perspective the significant drop between day one and day 3 results. Overall, as it currently stands further testing is required to truly know what is happening inside the cell from day 1 to day 3. From the optical images of the printed layers, it is evident that for designing a reliable device, it is required to focus on printing materials



that would not spread easily. This may need to change the ink formula for the electrode and electrolyte and/or conduct a treatment after printing each layer to produce a more solid structure. While this device isn't capable of real-world applications, it does provide proof of concept of the fabrication of a prototype energy storage device using a bioprinter.

Conclusions

This research outlined and tested a novel fabrication approach for creating EDLCs. The results were discussed at length to explore the feasibility of an idea such as this. Both fully printed and semiprinted cells were made. A technique to seal a cell was implemented for preserving the water in the gel electrolyte. While several different attempts were made to achieve reliable capacitive storage, the results proved inconclusive. Probable reasons for why the results were not as intended were discussed to gain a better insight into how bioprinting could be used to improve this prototype energy storage device fabrication. Overall, this research proved the relatively new and novel technique of bioprinting that can be applied in a manner many would not consider for traditional EDLC fabrication. This technique has the potential to bring about a new era of biodegradable eco-friendly fabrication.

Author contributions BS is the corresponding author of this work and can be reached at bseufert@uf.edu, Dr. AT and Dr. ST were the editors of this work.

Funding Funding support for Bianca Seufert was provided by NSF FGLSAMP BD: University of South Florida Florida-Georgia Louis

Stokes Alliance for Minority Participation (FGLSAMP) – HRD # 1906518.

Data availability Data will be made available upon request.

Declarations

Conflict of interests All authors claim no conflict of interest.

References

- Y. Gao et al., ChemPhysMater. (2022). https://doi.org/10.1016/j. chphma.2021.09.002
- L. Jiri et al., J. Energy Storage (2018). https://doi.org/10.1016/j. est.2018.03.012
- T. Pandhi et al., RSC Adv. (2020). https://doi.org/10.1039/D0RA0 4786D
- D. Costa et al., Micro Nano Syst. Lett. (2020). https://doi.org/10. 1186/s40486-020-0104-7
- A.A.K. Farizhandi et al., J. Mech. Behav. Biomed. Mater. (2020). https://doi.org/10.1016/j.jmbbm.2020.103960
- M. Duarte et al., Mater. Today Chem. (2021). https://doi.org/10. 1016/j.mtchem.2021.100617
- E. Axpe, M.L. Oyen, Int. J. Mol. Sci. (2016). https://doi.org/10. 3390/ijms17121976
- B. Aljafari et al., J. Solid State Chem. (2018). https://doi.org/10. 1007/s10008-018-4120-y

Publisher's Note Springer Nature remains neutral with regard to jurisdictional claims in published maps and institutional affiliations.

Springer Nature or its licensor (e.g. a society or other partner) holds exclusive rights to this article under a publishing agreement with the author(s) or other rightsholder(s); author self-archiving of the accepted manuscript version of this article is solely governed by the terms of such publishing agreement and applicable law.